FUNCTION

FUNCTION, 2021, 3(1): zqab053

https://doi.org/10.1093/function/zqab053
Advance Access Publication Date: 20 October 2021
Original Research

RESEARCH ARTICLE

Contribution of Postjunctional M2 Muscarinic Receptors to Cholinergic Nerve-Mediated Contractions of Murine Airway Smooth Muscle

Tuleen Alkawadri[1], Lorcan P McGarvey[2], ND Mullins[1], Mark A Hollywood[1], Keith D Thornbury[1], Gerard P Sergeant[1,*]

[1]Smooth Muscle Research Centre, Dundalk Institute of Technology, Dublin Road, Dundalk, Co. Louth, A91 K584, Ireland and [2]School of Medicine, Dentistry and Biomedical Sciences, Queen's University, Belfast, BT7 1NN, Northern Ireland

*Address correspondence to G.P.S. (e-mail: gerard.sergeant@dkit.ie)

Abstract

Postjunctional M2Rs on airway smooth muscle (ASM) outnumber M3Rs by a ratio of 4:1 in most species, however, it is the M3Rs that are thought to mediate the bronchoconstrictor effects of acetylcholine. In this study, we describe a novel and profound M2R-mediated hypersensitization of M3R-dependent contractions of ASM at low stimulus frequencies.. Contractions induced by 2Hz EFS were augmented by > 2.5-fold when the stimulus interval was reduced from 100 to 10 s. This effect was reversed by the M2R antagonists, methoctramine, and AFDX116, and was absent in M2R null mice. The M3R antagonist 4-DAMP abolished the entire response in both WT and M2R KO mice. The M2R-mediated potentiation of EFS-induced contractions was not observed when the stimulus frequency was increased to 20 Hz. A subthreshold concentration of carbachol enhanced the amplitude of EFS-evoked contractions in WT, but not M2R null mice. These data highlight a significant M2R-mediated potentiation of M3R-dependent contractions of ASM at low frequency stimulation that could be relevant in diseases such as asthma and COPD.

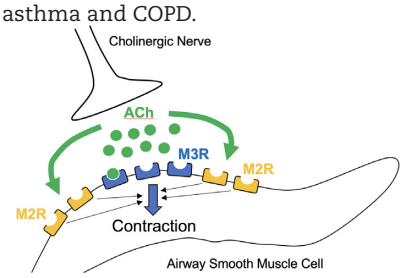

Key words: muscarinic; airways; smooth muscle; contraction; cholinergic; COPD

Submitted: 13 August 2021; **Revised:** 5 October 2021; **Accepted:** 18 October 2021

Introduction

Acetylcholine (ACh) released from parasympathetic nerves induces bronchoconstriction via activation of postjunctional muscarinic receptors (MRs) on airway smooth muscle (ASM).[1–3] Elevated cholinergic tone and sensitivity to cholinergic agonists is associated with chronic obstructive pulmonary disease (COPD)[4–6], thus, anticholinergic agents are used as a primary treatment option for this condition.[7] The bronchoconstrictor effect of ACh is widely regarded to be mediated by activation of M3 muscarinic receptors (M3Rs), even though they are outnumbered by M2Rs by a ratio of 4:1 in most species.[8–10] The exact role of the postjunctional M2Rs in ASM is still unclear, however prejunctional M2Rs located on parasympathetic nerve terminals in ASM act as autoinhibitory receptors that regulate cholinergic responses by suppressing ACh release.[2] Therefore, blockade of prejunctional M2Rs in ASM could, in theory, exacerbate airway obstruction via enhanced ACh release. Consequently, this has led to the pursuit of selective M3R antagonists for treatment of COPD that block the M3Rs responsible for bronchoconstriction, without affecting the autoinhibitory M2Rs that would enhance ACh output. For example, the M2/M3R antagonist tiotropium is favored over ipratropium as it dissociates more rapidly from M2Rs than M3Rs.[11]

Studies on small airways of M3R knockout mice showed that cholinergic responses were ∼60% smaller than wild-type controls, but were absent in mice that had both M2 and M3Rs knocked out, suggesting that both M2Rs and M3Rs are involved in cholinergic contractions of ASM.[12] Similarly, Semenov et al. showed that application of the M2R antagonist AFDX-116 inhibited contractions of murine trachea that were induced by submicromolar concentrations of carbachol (CCh).[13] Furthermore, they also reported that the threshold concentration for the inhibitory effects of AFDX116 strongly depended on the concentration of cholinergic agonist, increasing from 0.05 to 0.25 μM when the CCh concentration was increased from 0.5 to 3 μM. Similar findings were also reported by Unno et al., who found that M2R-dependent contractions of murine ileum were only evident at low agonist concentrations.[14] Therefore, it appears that M2R-dependent responses are more prevalent at lower agonist concentrations and that the contribution of postjunctional M2Rs to cholinergic contractions of ASM could be underestimated in studies that employ higher concentrations of cholinergic agonists or high nerve stimulation frequencies to induce contraction (eg 10–30 Hz).[15,16]

The primary aim of the present study was to reevaluate the contribution of M2Rs to nerve-evoked contractions of murine ASM. In particular, we examined responses induced at a low stimulus frequency (2 Hz). Our data demonstrate that, at 2 Hz EFS, there was a profound sensitization of the contractile response when the stimulus interval was shortened from 100 to 10 s. The sensitization was blocked by the M2R antagonists, methoctramine and AFDX116 and was absent in M2R-null mice. These data could have important consequences for our understanding of the role of MRs in ASM contraction and for the development of more effective treatment strategies for obstructive lung diseases.

Materials and Methods

Tissue Dissection

All procedures were carried out in accordance with current EU legislation and with the approval of Dundalk Institute of Technology Animal Use and Care Committee. Male and female C57BL/6 wild-type (WT) and B6N.129S4(Cg)-Chrm2 ^{tm1Jwe}/J, (M2R knock out) mice aged 10–16-weeks-old were humanely killed by intraperitoneal injection of pentobarbitone and the lungs were removed and placed in oxygenated Krebs solution. M2R knock out (M2R KO) mice were purchased from the Jackson Laboratory (Bar Harbor, Maine, USA). Homozygote M2R KOs were generated from the breeding of heterozygotes and were identified by genotyping using PCR as per JAX protocols and reagents. Confirmation that smooth muscle cells from M2R KO mice lacked M2Rs was provided by immunocytochemistry experiments, which showed that the robust immunofluorescence observed in wild-type ASM cells stained with M2R antibodies, was absent in M2R KOs (Figure S1). The bronchial tree was exposed by a sharp dissection under a microscope to remove surrounding blood vessels and lung tissue.[17] The left and right bronchi were removed and cut into rings and placed in Krebs solution.

Isometric Tension Recordings

Rings, 1–2 mm from the right and left main bronchi were mounted in water-jacketed organ baths, perfused with warmed Krebs solution, adjusted to 5 mN tension, and equilibrated for 40 min. Isometric contractions, were recorded using a Myobath system, and data acquired using DataTrax2 software (WPI). Mean contraction amplitude was measured by averaging peak contraction amplitude of 10 electric-field stimulation (EFS)-induced contractions during each parameter, or before and during drug addition (when they had their maximal effect). Drugs were added directly to the organ bath, where they were diluted in Krebs solution to their final concentration. Transmural nerve stimulation was applied via 2 platinum electrode wires (5 mm length and 2.5 mm apart) by a MultiStim system-D330 stimulator (Digitimer Ltd, England), which delivered 1 s trains of pulses (pulse amplitude 20 V, nominal; pulse duration 0.3 ms) at frequencies of 2 or 20 Hz, at intervals of 10 or 100 s. All EFS responses were blocked by application of tetrodotoxin (100 n; Figure S2). Experiments which compared responses in M2R KO mice with WT controls were performed at the same time.

Cell Dispersal and Immunocytochemistry

Single airway smooth muscle cells (ASMC) were isolated using a collagenase/proteinase mixture consisting of (per 5 mL of Hanks' Ca^{2+}-free solution) 15 mg collagenase (Sigma type 1a), 1 mg proteinase (Sigma type XXIV), 10 mg BSA (Sigma), and 10 mg trypsin inhibitor (Sigma) for ∼5 min at 37°C. They were then placed in Hanks' Ca^{2+}-free solution and stirred for a further 10–20 min to release single relaxed smooth muscle cells. These were stored in Hanks' Ca^{2+}-free solution (with Ca^{2+} added to a concentration of 100 μ) at 4°C. Coverslips (22 × 22 mm, #1.5, VWR) were prepared by treatment with poly-L lysine (Sigma Aldrich) for 30 min, followed by multiple washes with double distilled water. After coverslips were left to completely air-dry they were placed in a 6-well plate. A total of 150–200 μL of cellular suspension containing isolated ASMCs was pipetted onto each coverslip and allowed to settle for 45 min on ice. Cells were fixed in 2 mL of 2% paraformaldehyde (PFA, Sigma Aldrich) made up in phosphate buffered saline solution (PBS, Gibco) for 13 min at room temperature. Cells were washed 3 times with PBS for 5 min and permeabilized with 0.1% Triton X-100 (Sigma Aldrich) for 10 min at 4°C. In total, three 5-minute washes with PBS were performed prior to the blocking step, which required blocking the cells with SEA Block (Thermofischer) for 2 h at 4°C. Antibody incubation solution (20% SEA Block, 0.05% Triton X, and 1% BSA) was prepared and mixed with the primary antibodies (AntiCHRM2; 1:200 dilution, Atlas Antibodies; AntiCHRM3, 1:100 dilution, and Atlas Antibodies; smooth

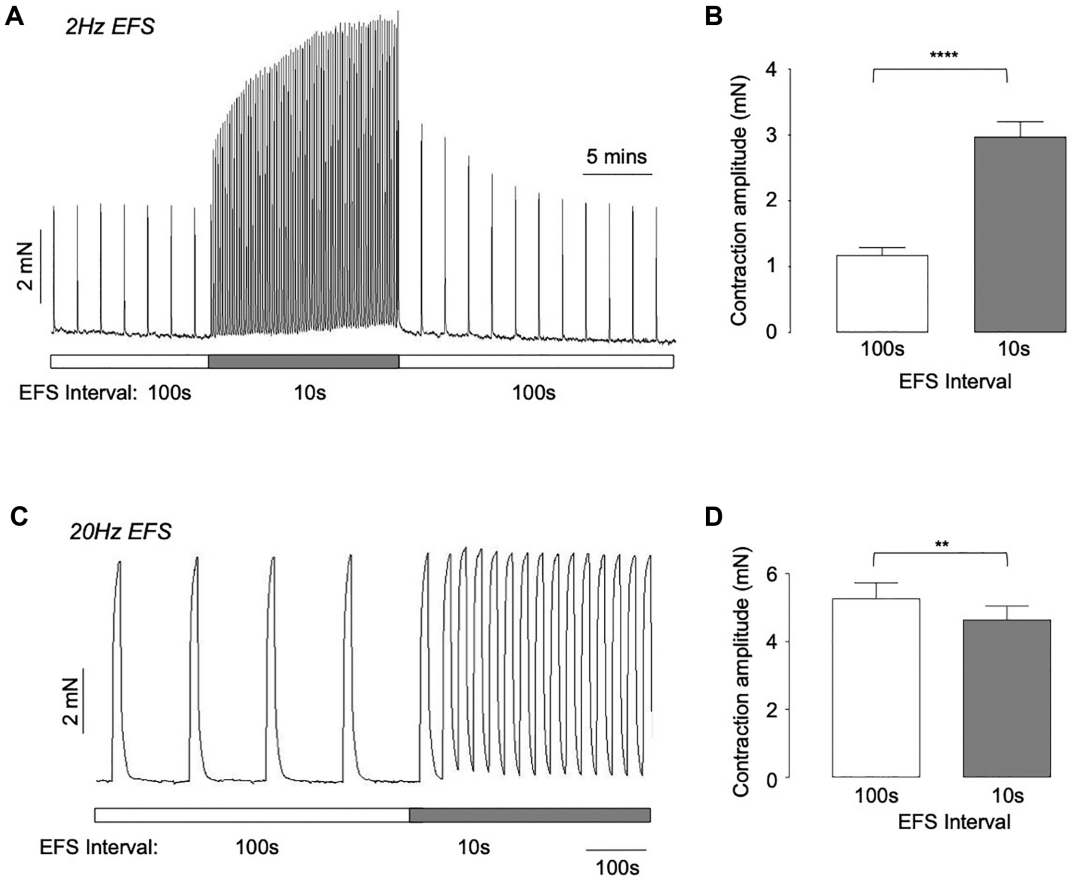

Figure 1. Reduction in stimulus interval enhances the amplitude of ASM contractions induced at 2 Hz, but not 20 Hz, EFS. (A) Representative trace showing that decreasing stimulus interval from 100 to 10 s increased the amplitude of contractions of murine bronchial rings evoked by 2 Hz EFS. (B) Summary plot of mean peak contraction amplitude (2 Hz EFS) at 100 s (open bar) and 10 s (shaded bar) intervals ($n = 46$, $N = 32$, $P < .0001$). (C) Representative trace showing that contractions of murine bronchial rings evoked by 20 Hz EFS were not augmented by a reduction in stimulus interval from 100 to 10 s. (D) Summary plot of mean peak amplitude of EFS-evoked contractions (20 Hz) at 100 s (open bar) and 10 s (shaded bar) intervals ($n = 13$, $N = 8$, $P < .01$. Error bars represent SEM. ** and **** denote $P < .01$ >, and $P < .0001$, respectively.

muscle α actin. 1:100 dilution, Dako). A total of 50 μL of the primary antibody solution was pipetted onto the antibody tray and coverslips were carefully placed using forceps. Antibody trays were transferred to a glass megadish and the antibodies were left to incubate overnight at 4°C. The coverslips were removed from the antibody trays and placed in the 6-well plate, where the primary antibody was removed by three 5-minute washes with 20% SEA Block. Secondary antibody solution (Alexa Fluor 488, 1:1000 dilution (Invitrogen) and Alexa Fluor 555, 1:1000 (Life Technologies) in PBS) was pipetted onto the antibody trays and the coverslips were carefully placed using forceps. Cells were incubated in secondary antibodies for 2 h in the dark at room temperature. Coverslips were placed back in the 6-well plates and the cells were washed with ice cold PBS for 4 times for 5 min. A drop of a mounting medium (VectaShield, Vector Laboratories) was added to slides (0.8–1 mm, VWR) labeled with the respective antibodies, and the coverslips were carefully placed on the slides and sealed using nail varnish. Control coverslips were simultaneously prepared by omitting the primary antibody incubation step (secondary antibody only). Control dishes were imaged using the same experimental parameters for each image to ensure no positive immunoreactivity occurred. Immunofluorescence of isolated ASMCs was imaged with an Olympus IX31 microscope (Olympus-life science) using an oil-immersed 60x objective lens. Using a laser, excitation wavelengths of 488 and 561 nm were used to visualize immunoreactivity in the cells. Using ImageJ (version 1.48, National Institute of Health, MD) software, 10-second videos and snaps were obtained from cells and analyzed.

Drugs and Solutions

4-DAMP, AFDX-116, tetrodotoxin (Tocris), carbachol, methoctramine (Sigma Aldrich), and indomethacin (Abcam) were solubilized in DMSO, ethanol, or distilled water. Krebs solution was composed of (mM) 120 NaCl, 5.9 KCl, 25 $NaHCO_3$, 1.2 $NaH_2PO_4{\cdot}2H_2O$, 5.5 glucose, 1.2 $MgCl_2$, and 2.5 $CaCl_2$. pH was adjusted to 7.4 by bubbling the solution with 95% O_2–5% CO_2.

Data Analysis and Statistics

Experimental series were obtained from 4 or more animals; n refers to the number of tissue strips studied and N to the number of animals. Data were analyzed using Prism software (GraphPad). Summary data are presented as mean ± SEM. Statistical comparisons were performed on original (non-normalized) data using either Student's paired t-test or, if 3 experimental groups were compared, ANOVA followed by Bonferonni post hoc test, with $P < 0.05$ > considered statistically significant.

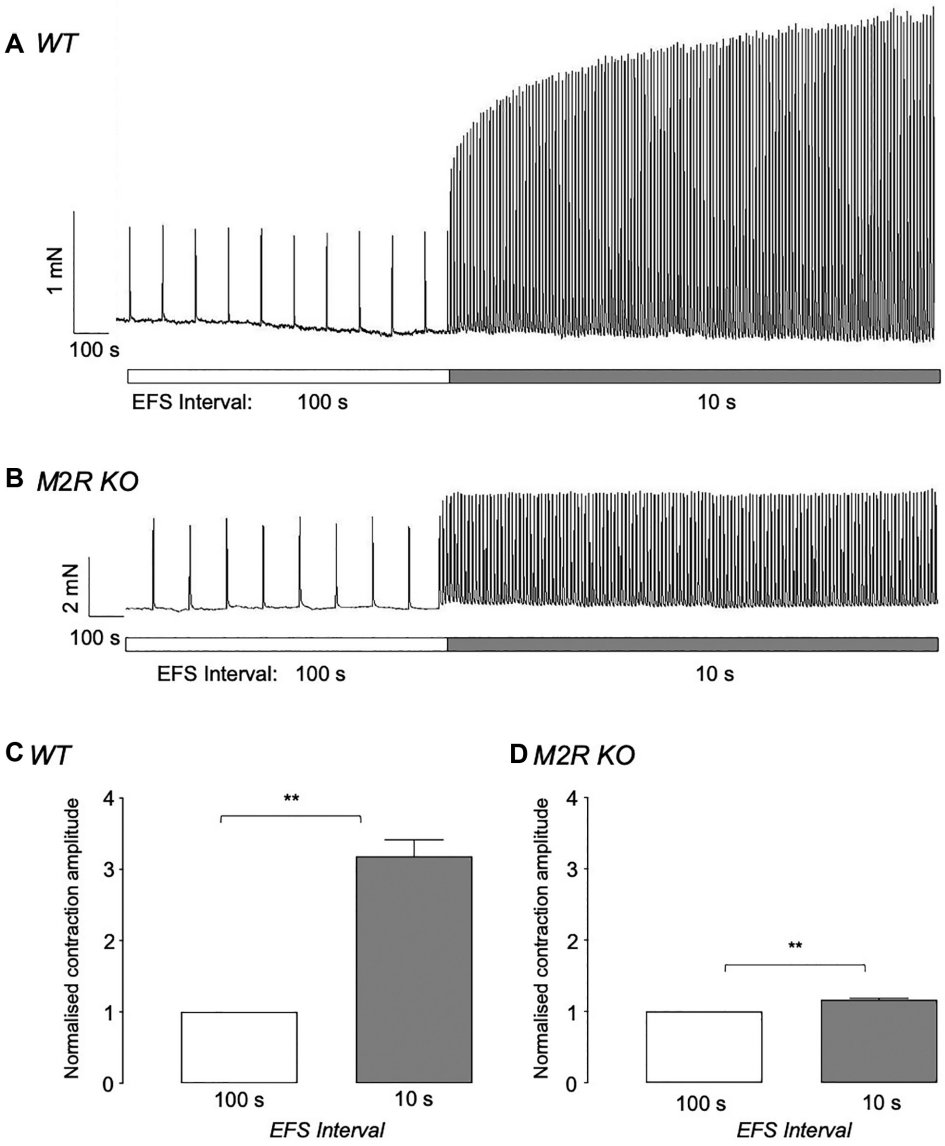

Figure 2. Potentiation of ASM contractions induced by a reduction in stimulus interval is absent in M2R knock out mice. (A) Representative trace from a wild type (WT) mouse showing that a reduction in stimulus interval from 100 to 10 s increased the amplitude of contractions of murine bronchial rings evoked by 2Hz EFS. (B) Representative trace from an M2R knock out (KO) mouse showing that a reduction in stimulus interval from 100 to 10 s only slightly increased the amplitude of contractions of murine bronchial rings evoked by 2 Hz EFS. (C) and (D) Summary plots of mean peak contraction amplitude (2 Hz EFS) at 100 s (open bar) and 10 s (shaded bar) intervals in WT (C) and M2R KO mice (D). Error bars represent SEM. ** denotes $P < .01$.

Results

Effect of Stimulus Parameters on EFS-evoked Contractions of Murine Bronchial Rings

Repetitive EFS (frequency 2 Hz, duration 10 s, and 100 s intervals) of murine bronchial rings induced robust and consistent contractions. These responses were inhibited by tetrodotoxin (TTX (100 nM); Figure S2), confirming that these responses were neurogenic in origin. When the interval between stimulation was reduced from 100 to 10 s, contraction amplitude increased (Figure 1A). In 46 preparations, reducing the stimulus interval from 100 to 10 s increased mean contraction amplitude > 2.5-fold, from 1.18 ± 0.11 to 2.97 ± 0.23 mN ($n = 46$, $N = 32$, $P <$ .0001; Figure 1B). When this protocol was repeated using a higher stimulus frequency (20 Hz), no increase in contraction amplitude was observed, indeed the mean amplitude of contraction was reduced from 5.27 ± 0.46 mN at 100 s intervals, to 4.65 ± 0.4 mN at 10 s intervals ($P < .01>$, $n = 13$, $N = 8$; Figure 1C and D). Therefore, cholinergic nerve-mediated contractions of ASM were potentiated by a reduction in stimulus interval, but this was only evident at low stimulus frequencies and not at higher frequencies which have been used in other studies to characterize nerve-mediated contractions of ASM.[18]

Contribution of M2Rs to Potentiation of EFS-evoked Contractions of Murine Bronchial Rings

To examine if the augmented cholinergic contractions induced by reduction in stimulus interval involved activation of M2Rs, responses were compared in WT and M2R null mice (Figure 2A and B, respectively). It was clear that the large potentiation of EFS-evoked contractions observed in WT mice (Figures 1A

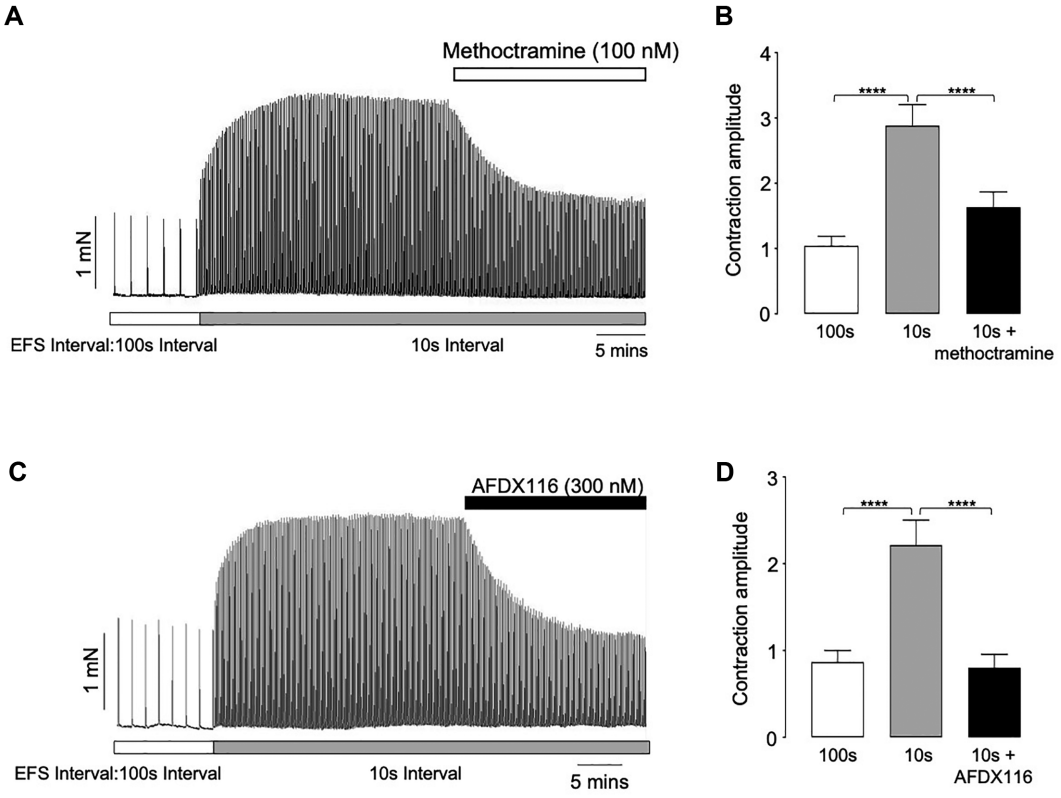

Figure 3. M2R antagonists, methoctramine and AFDX116, reverse the potentiation of EFS-evoked contractions, induced by a reduction in stimulus interval, in WT mice. (A) Representative trace from a wild type (WT) mouse showing that methoctramine (100 nM) reversed the increase in contraction amplitude induced by reduction in stimulus interval from 100 to 10 s. (B) Summary bar chart plotting mean contraction amplitude under control conditions at 100 and 10 s intervals and in the presence of methoctramine at 10 s intervals. (C) Representative trace from a wild type (WT) mouse showing that AFDX116 (300 nM) reversed the increase in contraction amplitude induced by reduction in stimulus interval from 100 to 10 s. (D) Summary bar chart plotting mean contraction amplitude under control conditions at 100 and 10 s intervals and in the presence of AFDX116 at 10 s intervals. Error bars represent SEM. **** denote $P < .0001$

and 2A) was not evident in mice lacking M2Rs. Summary data presented in Figure 2C and D, respectively, shows that mean contraction amplitude in WT mice increased by > 218% ($n = 9$, $N = 4$, $P < .01$>) compared to 19% in M2R KO mice ($n = 10$, $N = 4$, $P < .01$>).

Next, experiments were performed to examine if the augmented responses in WT mice were affected by the selective M2R antagonists methoctramine (100 nM) and AFDX116 (300 nM). The representative traces in Figure 3A and C, respectively, show that each drug reversed the increase in contraction amplitude induced upon reduction in stimulus interval from 100 to 10 s. The summary plots in Figure 3B and D show mean contraction amplitude at 100 s and 10 s intervals, before and during application of methoctramine and AFDX116, respectively. Methoctramine significantly reduced contraction amplitude by 45% from 2.9 ± 0.3 to 1.6 ± 0.2 mN ($P < .0001$, $n = 24$, $N = 18$) and AFDX116 reduced mean contraction amplitude by 64% from 2.2 ± 0.3 to 0. ± 0.15 mN ($P < .0001$, $n = 18$, $N = 15$). Methoctramine did not affect contractions evoked at 100 s intervals (Figure S3).

In order to examine if the inhibitory effects of methoctramine (100 nM) and AFDX116 (300 nM) resulted from off target actions, not involving M2Rs, their effects were examined on M2R KO mice. Figure 4 compares the effect of methoctramine (100 nM) on EFS-evoked contractions of ASM (2 Hz, 10 s interval) in WT (Figure 4A) and M2R KO mice (Figure 4B). Responses in WT mice were attenuated by methoctramine, whereas contractions in M2R KO mice were unaffected. Summary data in Figure 4C and D shows that methoctramine reduced mean contraction amplitude in WT mice by 63%, from 1.33 ± 0.3 to 0.49 ± 0.2 mN ($n = 6$, $N = 5$, $P < .001$), but did not affect responses in M2R KO mice ($n = 7$, $N = 4$, ns). Similarly, AFDX-116 failed to inhibit contractions in M2R KO mice (Figure 5B). Summary data in Figure 5C and D show that mean contraction amplitude of ASM taken from WT mice was reduced by 66% in the presence of AFDX-116 (from 1.32 ± 0.3 to 0.45 ± 0.18 mN, $n = 4$, $N = 4$, $P < .05$>; Figure 5C), whereas no significant effects occurred in M2R KO preparations ($n = 9$, $N = 4$, ns, Figure 5D).

To investigate the contribution of M3Rs to EFS-induced contractions of ASM we examined the effect of the M3R antagonist, 4-DAMP (3nM). Data in Figure 6 shows that 4-DAMP abolished EFS (2 Hz, 10 s interval) -evoked contractions in both WT ($n = 8$, $N = 6$) and M2R KO ($n = 9$, $N = 4$) mice. Therefore, although a reduction in stimulus interval potentiated contraction amplitude via activation of M2Rs, there was an absolute requirement for M3Rs to initiate these responses.

We reasoned that the M2R-mediated potentiation of nerve-evoked contractions of ASM, at short stimulus intervals, could be due to a small increase in ACh levels, and tested this idea by examining the effect of a sub-threshold concentration of CCh on EFS-evoked contractions at long (100 s) intervals. CCh (10 nM) enhanced contraction amplitude in WT mice and this

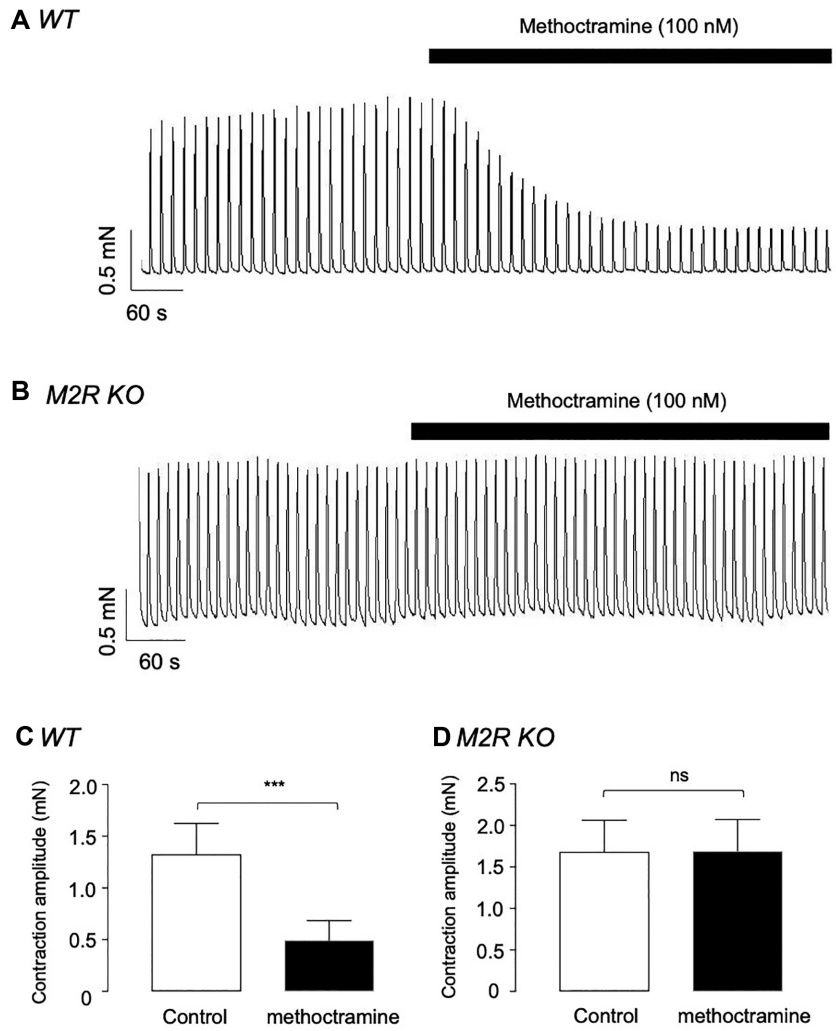

Figure 4. Inhibitory effects of methoctramine on EFS-evoked contractions of ASM are absent in M2R KO mice. (A) and (B) Representative traces from a wild type (WT) and M2R KO mouse, respectively, showing that methoctramine (100 nM) inhibited EFS-evoked (2Hz, 10s intervals) contractions in WT (A), but not M2R KO mice (B). C & D) Summary plots of mean contraction amplitude under control conditions and in the presence of methoctramine in WT (C) and M2R KO (D) mice. Error bars represent SEM. *** denote $P < .001$.

effect was reversed by application of methoctramine (Figure 7A). In 7 preparations, CCh enhanced mean contraction amplitude by 55.5%, from 2.25 ± 0.28 to 3.5 ± 0.4 mN ($n = 7$, $N = 4$, $P < .0001$) and addition of methoctramine reduced mean amplitude to 2.45 ± 0.4 mN ($n = 7$, $N = 4$, $P < .001$). However, in bronchial rings taken from M2R KO mice, CCh (10 nM) application produced a much smaller increase in contraction amplitude of 11% ($n = 9$, $N = 4$, $P < .05$>; Figure 7C and D). Therefore, the potentiating effects of CCh on EFS-evoked contractions in WT mice were reversed by methoctramine and were greatly diminished in M2R KO mice. We also found that contractions of murine ASM induced by the acetylcholinesterase inhibitor, neostigmine (1 μ), were inhibited by methoctramine (100 nM). The representative trace and summary data in Figure S5 show that neostigmine induced robust contraction of ASM and that methoctramine reduced these responses from 4.8 ± 0.75 to 1.99 ± 0.73 mN ($P < .01$>, $n = 6$, $N = 5$).

Discussion

The results of the present study demonstrate that postjunctional M2Rs make a greater contribution to cholinergic nerve-induced bronchoconstriction than previously realized. Using low frequency EFS (2 Hz), we demonstrated that activation of M2Rs sensitized ASM to M3R stimulation, resulting in a doubling of the force of M3R-dependent contractions. This represents a paradigm shift in our understanding of the mechanisms that regulate ASM contraction and brings into question the logic of excluding antimuscarinic drugs that affect M2Rs as potential therapeutic options for treatment of obstructive lung conditions.

M2Rs are G_i-protein-coupled receptors that reduce intracellular cAMP levels via inhibition of adenylate cyclase[19] and are known to be involved in cholinergic-mediated contractions of the stomach, ileum, and bladder.[20] However, despite their relatively high expression levels in ASM, and studies which indicate that their activation can induce ASM contraction[21,22], the consensus is that M2Rs are not involved in cholinergic nerve-mediated contractions of the airways.[2] Instead, it is generally accepted that activation of postjunctional M2Rs can provide a functional antagonism to β-adrenoceptor (β-AR)-induced relaxations of ASM by counteracting the rise in cAMP levels induced by β-AR activation.[10,12,23–25] In the present study, we showed that nerve-evoked contractions of ASM, at low stimulus frequencies, were potentiated by a reduction in stimulus interval. This effect was reversed by the M2R antagonists methoctramine and AFDX116, and was absent in M2R KO mice.

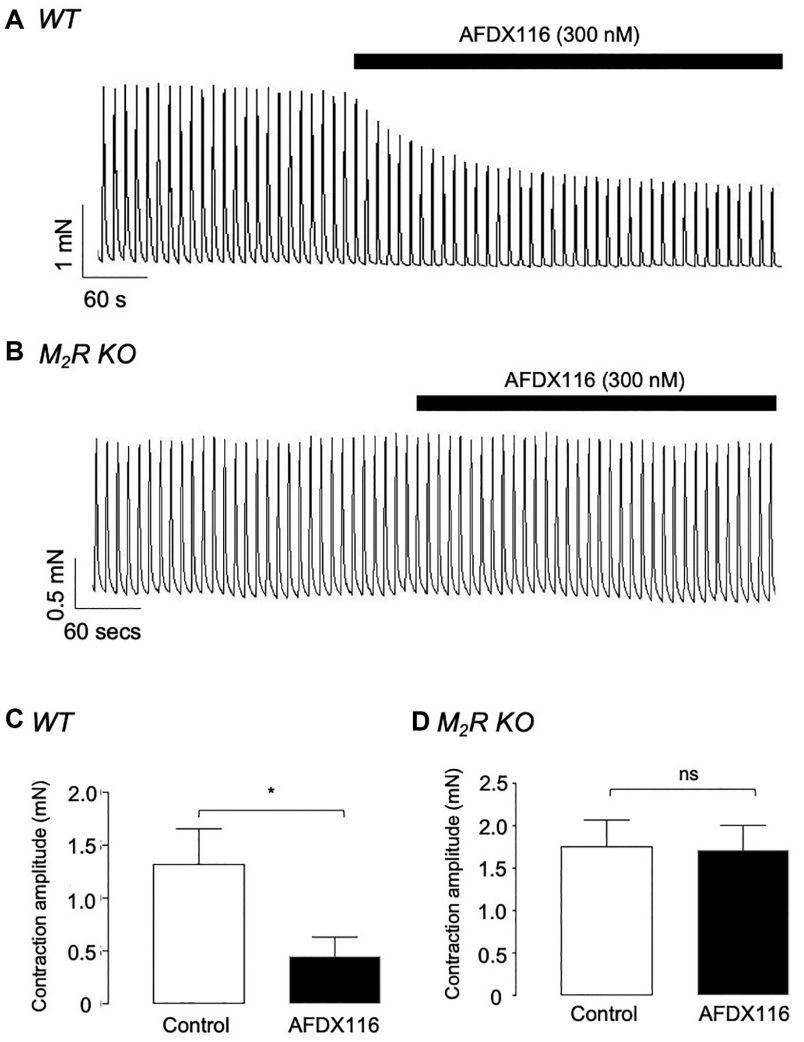

Figure 5. Inhibitory effects of AFDX116 on EFS-evoked contractions of ASM are absent in M2R KO mice. (A) and (B) Representative traces from a wild type (WT) and M2R KO mouse, respectively, showing that AFDX116 (300 nM) inhibited EFS-evoked (2 Hz, 10 s intervals) contractions in WT (A), but not M2R KO mice (B). (C) and (D) Summary plots of mean contraction amplitude under control conditions and in the presence of AFDX116 in WT (C) and M2R KO (D) mice. Error bars represent SEM. * denote $P < .05$.

In contrast, the M3R antagonist 4-DAMP abolished the entire contraction. These data support the idea that M3Rs are essential for cholinergic contractions of ASM, but that M2Rs act in concert to augment the M3R-dependent contractions. This concept was noted previously by Ehlert, who reported that M2Rs could exert "low potency potentiation of the contractile response to M3 receptor activation" and that activation of M2Rs could enhance M3R-mediated contractions in asthma.[20] However, our findings show that the contribution of postjunctional M2Rs to cholinergic contractions of ASM is much greater than previously realized and that M2R blockers reduced cholinergic contractions, rather than enhancing them due to block of prejunctional M2Rs. However, we also demonstrated that, under different experimental conditions (20 Hz EFS, 100 s intervals, Figure S4), application of the M2R antagonist methoctramine could enhance these responses, as described previously.[2] Therefore, the contribution of postjunctional M2Rs to ASM contraction is highly dependent on the stimulus parameters used and may have been missed in previous studies that used high stimulus frequencies and high agonist concentrations.

The results of the present study show that subtle changes to stimulus parameters can elicit profound changes on the contractile response of ASM and this could be very important in terms of airway hyperresponsiveness and the pathogenesis of obstructive lung disorders. In intestinal smooth muscle, it has been reported that M2Rs primarily contribute to contractions induced by low agonist concentrations, while M3Rs dominate at higher concentrations[26] and similar findings have been reported in ASM.[13,14] Such findings are consistent with the lack of involvement of M2Rs in responses induced by 20Hz EFS in the present study. However, we found that contractions elicited by low frequency (2 Hz) EFS, at 100 s intervals were unaffected by the M2R antagonists, methoctramine and AFDX-116, but were abolished by the M3R antagonist 4-DAMP, indicating that M3Rs can dominate even at low stimulus frequencies. It was only when the stimulus interval was decreased that the M2R component became apparent. This effect was mimicked by application of a low, sub-threshold, concentration (10 nM) of CCh, therefore, the potentiating effects induced by reduction in stimulus interval, could be associated with a small increase in the ambi-

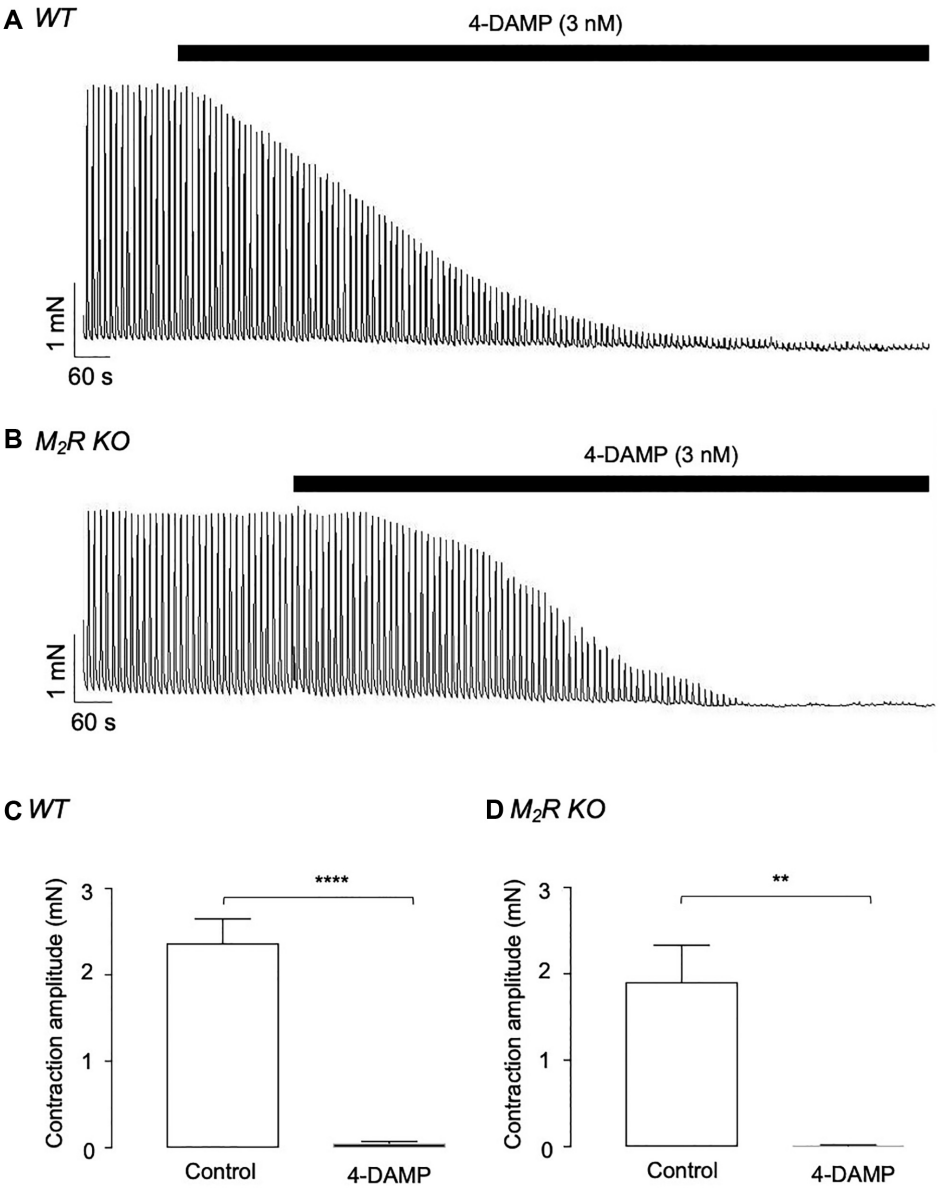

Figure 6. The M3R antagonist, 4-DAMP, abolishes EFS-evoked contractions in wild-type and M2R-KO mice. (A) and (B) Representative traces from a wild type (WT) and M2R KO mouse, respectively, showing that 4-DAMP (3 nM) abolished EFS-evoked (2 Hz, 10 s intervals) contractions in WT (A) and M2R KO mice (B). (C) and (D) Summary plots of mean contraction amplitude under control conditions and in the presence of 4-DAMP in WT (C) and M2R KO (D) mice. Error bars represent SEM. ** and **** denote $P < .01 >$ and $P < .0001$, respectively.

ent ACh concentration. These findings are consistent with a model in which M3Rs are located at nerve-smooth muscle junctions and represent the primary target for neuronally released ACh, whereas M2Rs are located extrajunctionally and are activated by small increases in the ambient ACh concentration. This idea is reinforced by the finding that application of the acetylcholinesterase inhibitor neostigmine induced contractions that were inhibited by methoctramine. It is also analogous to the situation in the murine stomach whereby ACh released from motor nerves primarily targets M3Rs on interstitial cells of Cajal, but that overflow of ACh can bind to extrajunctional MRs on smooth muscle cells.[27,28]

Further investigation is required to elucidate the mechanisms that underlie activation of M2Rs in ASM. ACh can be released from several cell types in the airways, including epithelial cells and lymphocytes, which both possess the components required for ACh synthesis.[29] However, since the responses in this study were abolished by tetrodotoxin, it appears likely that the source of ACh responsible for the augmented contractions induced by reduction in stimulus interval was neuronal in origin. It is tempting then to speculate that the potentiation of contraction amplitude resulted from overspill of junctional ACh, leading to activation of extrajunctional M2Rs. However, this would require saturation of junctional acetylcholinesterase enzymes which, given the their very high catalytic activity[30], would require high ACh levels, normally associated with long duration and high frequency stimulation. For example, Bhetwal et al., showed that bath applied CCh to the murine gastric fundus increased CPI-17 and MYPT1 phosphorylation, whereas EFS (5–20 Hz, for 5–30 s duration) only increased CPI-17 phosphorylation.[28] However, when acetylcholinesterase enzymes were inhibited EFS elicited similar responses to CCh demonstrating

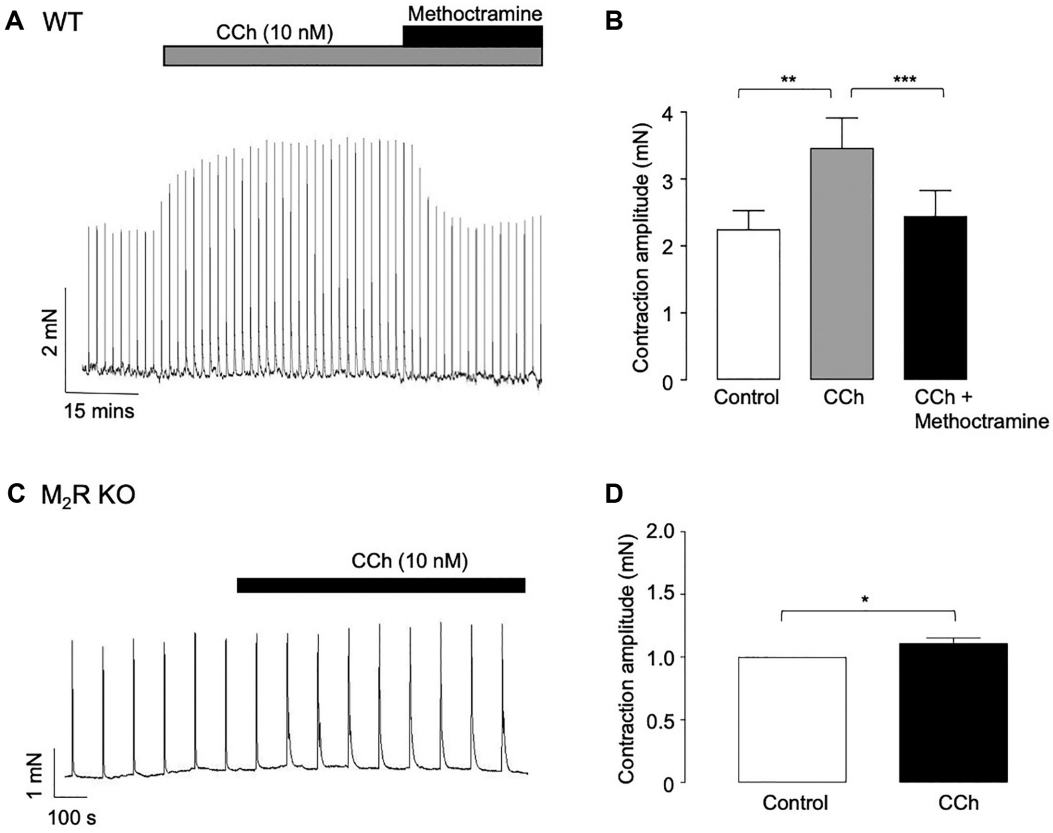

Figure 7. CCh-induced potentiation of EFS-evoked contractions is dependent on activation of M2Rs. (A) Representative trace from a WT mouse showing that CCh (10 nM) enhanced the amplitude of EFS-evoked contractions (2 Hz, 100 s intervals) of ASM in WT mice, and this effect was reversed by application of methoctramine. (B) Summary plot showing mean contraction amplitude of EFS-evoked contractions under control conditions, in the presence of CCh and in the presence of CCh plus methoctramine. (C) Representative trace from an M2R KO mouse showing that CCh (10 nM) did not enhance the amplitude of EFS-evoked contractions (2 Hz, 100 s intervals). (D) Summary plot of mean contraction amplitude before and during the presence of CCh in bronchial rings taken from M2R KO mice. Error bars represent SEM. *, ** and **** denote $P < .05>$, $P < .01 >$, and $P < .0001$, respectively.

that, even at higher frequency and longer duration EFS, acetylcholinesterase enzymes prevented neurally-released ACh from activating MRs located on the bulk smooth muscle. Therefore, it appears unlikely that the stimulus parameters employed in the present study (2 Hz, 1 s duration, 10 s intervals) would be capable of producing enough ACh to overwhelm the ACh clearance mechanisms required to induce overspill of junctional ACh.

Kajekar et al., reported 2 different types of human bronchial parasympathetic ganglia neurons, based on distinct action potential firing patterns (tonic and phasic) in response to depolarizing stimuli. It was found that the threshold for activating phasic neurons was 2.2-fold higher than tonic neurons.[31] Therefore, it is possible that changes to the stimulus interval in the present study resulted from activation of a greater number of cholinergic neurons, which would increase the probability of M2R activation. An alternative hypothesis is that both M2 and M3Rs are located junctionally and that the enhanced responses result from a functional synergism between both receptors. In ileal smooth muscle, it has been reported between M2 and M3Rs are tightly connected and that activation of both receptors is required to activate a non-selective cation current referred to as $mI_{cat.}$[32] Such a mechanism fits with the effects of M2 and M3R antagonists on the potentiated responses described in the present study. However, if both receptors are closely associated at nerve-smooth muscle junctions it is unclear why M2Rs were not involved in responses to EFS at 100 s intervals. It is clear that further investigation is required to unravel these issues.

The cellular mechanisms that underlie M2R-dependent contraction of ASM also require further investigation. ASMC possess plasmalemmal voltage-dependent Ca^{2+} channels (VDCC) [33,34], however, there is a lack of consensus as to the role played by membrane potential and VDCC in contraction of ASM in response to agonist stimulation.[13,35,36] Nevertheless, studies have shown the stimulation of MRs can lead to closure of BK channels[22] and activation of mI_{cat}[37] that would both tend to depolarize membrane potential and activate VDCC. In the ileal smooth muscle cells, mI_{cat} is mediated by TRPC4 channels[38], whereas TRPC3 channels have been reported to account for mI_{cat} in ASMC.[39] While activation of mI_{cat} would be expected to induce depolarization and stimulate Ca^{2+} influx via VDCCs, it may also have hyperpolarizing effects as a result of accumulation of intracellular Na^+, increasing the activity of the Na^+/K^+ pump.[40] If M2R-dependent contractions of ASM are dependent on Ca^{2+} influx via VDCC then it is possible that these responses could be suppressed by Ca^{2+}-induced inactivation of Ca^{2+} channels following IP_3-mediated Ca^{2+} release from intracellular Ca^{2+} stores, as is the case in intestinal smooth muscle.[41] This may explain why M2R-dependent responses were not apparent at higher stimulation frequencies in the present study.

Reducing the stimulus frequency in M2R KO preparations resulted in a small (19%) increase in contraction amplitude, compared to that observed in WT controls (218% increase). These responses were abolished by 4-DAMP indicating that they were reliant on activation of M3Rs. In addition, although the amplitude of contractions induced by a decrease in stimulus interval in WT tissues was greatly diminished by methoctramine, they were still at slightly elevated level compared to control. Therefore, these data leave open the possibility that a small proportion of the enhancement of contraction amplitude may be due to stimulation of M3Rs. However, it is also possible that methoctramine did not maximally block M2Rs at the concentration used and that these responses were still M2R-dependent. Furthermore, it was notable that the small increase in contraction amplitude in M2R KO tissues was associated with an increase in tone, which was not observed in WT tissues. Reasons for this difference are unclear but may reflect compensatory changes in the M3R pathway when M2R expression is ablated and could affect responses to EFS.

Our conclusions on the role of M2Rs in ASM are, in part, dependent on the selectivity of the M2R antagonists used in this study. Methoctramine binds to M2Rs with high affinity[42] and M3Rs with low affinity[43] and Melchiorre et al., reported a 100-fold separation between the effects of methoctramine on M2 vs. M3Rs.[42] Jakubik et al., noted that the negative logarithm of inhibition constants (pKi) for methoctramine on M2Rs vs. M3Rs were 7.29 and 5.69, respectively.[44] Similarly, AFDX-116 also showed high selectivity for M2Rs over M3Rs with pKi values of 7.18 vs. 5.28, respectively.[44] Therefore, at the concentrations used in this study, the effects of these drugs are consistent with an effect on M2Rs. In addition, since these drugs failed to inhibit EFS-evoked contractions in M2R KO mice, it seems highly likely that their effects in WT mice are brought about by selective block of M2Rs. In contrast, 4-DAMP poorly discriminates between M3R and M2Rs (pKi values of 8.5 and 7.72, respectively[44], opening up the possibility that some responses attributed to M3Rs in this study may be caused by inhibition of M2Rs. Nevertheless, given the low concentration used in this study (3 nM) and the similarity of the effects of 4-DAMP in WT and M2R KO mice, it seems most likely that the effects of 4-DAMP were due to inhibition of M3Rs.

In summary, we report a novel and profound M2R-mediated hypersensitization of M3R-dependent contractions of ASM at low stimulus frequencies and intervals. We speculate that a small increase in ambient ACh concentration, possibly from non-neuronal sources, could be a causative factor in the generation of airway hyperresponsiveness in diseases such as asthma and COPD.

Supplementary Material

Supplementary material is available at the *APS Function* online.

Acknowledgments

The authors are grateful for technical support provided by Billie McIlveen.

Author Contributions

TA completed all experiments, drafted figures, performed statistical analyses, contributed to study design and data interpretation, and manuscript review. LMcG MH, NM, LMcG and KT contributed to study design, data interpretation, and manuscript review. GS wrote the paper, drafted figures, contributed to study design and data interpretation, and manuscript review.

Funding

This work was supported by the BREATH project, funded by the European Union Interreg VA Health and Life Science Programme. INT-VA/045

Competing Interests

No Conflicts of Interest.

Data Availability

The data underlying this article will be shared on reasonable request to the corresponding author.

References

1. Zaagsma J, Roffel AF, Meurs H. Muscarinic control of airway function. *Life Sci* 1997;**60**(13-14):1061–1068.
2. Fryer AD, Jacoby DB. Muscarinic receptors and control of airway smooth muscle. *Am J Respir Crit Care Med* 1998;**158**(supplement_2):S154–S160.
3. Barnes PJ. Muscarinic receptor subtypes in airways. *Life Sci* 1993;**52**(5-6):521–527.
4. Gross NJ, Skorodin MS. Role of the parasympathetic system in airway obstruction due to emphysema. *N Engl J Med* 1984;**311**(7):421–425.
5. Gross NJ, Co E, Skorodin MS. Cholinergic bronchomotor tone in COPD. Estimates of its amount in comparison with that in normal subjects. *Chest* 1989;**96**(5):984–987.
6. Gosens R, Zaagsma J, Meurs H, Halayko AJ. Muscarinic receptor signaling in the pathophysiology of asthma and COPD. *Respir Res* 2006;**7**(1):73.
7. Cazzola M, Page CP, Calzetta L, Matera MG. Pharmacology and therapeutics of bronchodilators. *Pharmacol Rev* 2012;**64**(3):450–504.
8. Haddad EB, Mak JC, Hislop A, Haworth SG, Barnes PJ. Characterization of muscarinic receptor subtypes in pig airways: radioligand binding and northern blotting studies. *Am J Physiol* 1994;**266**(6 Pt 1):L642–8.
9. Roffel AF, Elzinga CR, Van Amsterdam RG, De Zeeuw RA, Zaagsma J. Muscarinic M2 receptors in bovine tracheal smooth muscle: discrepancies between binding and function. *Eur J Pharmacol* 1988;**153**(1):73–82.
10. Fernandes LB, Fryer AD, Hirshman CA. M2 muscarinic receptors inhibit isoproterenol-induced relaxation of canine airway smooth muscle. *J Pharmacol Exp Ther* 1992;**262**(1):119–26.
11. Spina D. Current and novel bronchodilators in respiratory disease. *Curr Opin Pulm Med* 2014;**20**(1):73–86.
12. Struckmann N, Schwering S, Wiegand S, et al. Role of muscarinic receptor subtypes in the constriction of peripheral airways: studies on receptor-deficient mice. *Mol Pharmacol* 2003;**64**(6):1444–1451.
13. Semenov I, Wang B, Herlihy JT, Brenner R. BK channel β1 subunits regulate airway contraction secondary to M2 muscarinic acetylcholine receptor mediated depolarization. *J Physiol* 2011;**589**(7):1803–1817.
14. Unno T, Matsuyama H, Sakamoto T, et al. M(2) and M(3) muscarinic receptor-mediated contractions in longitudinal

smooth muscle of the ileum studied with receptor knockout mice. *Br J Pharmacol* 2005;**146**(1):98–108.
15. Fryer AD, Maclagan J. Muscarinic inhibitory receptors in pulmonary parasympathetic nerves in the guinea-pig. *Br J Pharmacol* 1984;**83**(4):973–978
16. Ito Y, Yoshitomi T. Autoregulation of acetylcholine release from vagus nerve terminals through activation of muscarinic receptors in the dog trachea. *Br J Pharmacol* 1988;**93**(3):636–646.
17. Bradley E, Large RJ, Bihun VV, et al. Inhibitory effects of openers of large-conductance Ca^{2+}-activated K+ channels on agonist-induced phasic contractions in rabbit and mouse bronchial smooth muscle. *Am J Physiol Cell Physiol* 2018;**315**(6):C818–C829.
18. Kilbinger H, Schneider R, Siefken H, Wolf D, D'Agostino G. Characterization of prejunctional muscarinic autoreceptors in the guinea-pig trachea. *Br J Pharmacol* 1991;**103**(3): 1757–1763.
19. Ehlert FJ, Ostrom RS, Sawyer GW. Subtypes of the muscarinic receptor in smooth muscle. *Life Sci* 1997;**61**(18): 1729–1740.
20. Ehlert FJ. Contractile role of M2 and M3 muscarinic receptors in gastrointestinal, airway and urinary bladder smooth muscle. *Life Sci* 2003;**74**(2-3):355–366.
21. Hirshman CA, Lande B, Croxton TL. Role of M2 muscarinic receptors in airway smooth muscle contraction. *Life Sci* 1999;**64**(6-7):443–448.
22. Kume H, Mikawa K, Takagi K, Kotlikoff MI. Role of G proteins and KCa channels in the muscarinic and beta-adrenergic regulation of airway smooth muscle. *Am J Physiol* 1995;**268**(2 Pt 1):L221–9.
23. Fayon M, Dumas De La Roque E, Berger P, et al. Increased relaxation of immature airways to beta2-adrenoceptor agonists is related to attenuated expression of post-junctional smooth muscle muscarinic M2 receptors. *J Appl Physiol* 2005;**98**(4):1526–1533.
24. Brown SM, Koarai A, Sturton RG, Nicholson AG, Barnes PJ, Donnelly LE. A role for M(2) and M(3) muscarinic receptors in the contraction of rat and human small airways. *Eur J Pharmacol* 2013;**702**(1-3):109–115.
25. Sarria B, Naline E, Zhang Y, et al. Muscarinic M2 receptors in acetylcholine-isoproterenol functional antagonism in human isolated bronchus. *Am J Physiol Lung Cell Mol Physiol* 2002;**283**(5):L1125–L1132.
26. Sakamoto T, Unno T, Kitazawa T, et al. Three distinct muscarinic signalling pathways for cationic channel activation in mouse gut smooth muscle cells. *J Physiol* 2007;**582**(1): 41–61.
27. Sung TS, Hwang SJ, Koh SD, et al. The cells and conductance mediating cholinergic neurotransmission in the murine proximal stomach. *J Physiol* 2018;**596**(9):1549–1574.
28. Bhetwal BP, Sanders KM, An C, Trappanese DM, Moreland RS, Perrino BA. Ca^{2+} sensitization pathways accessed by cholinergic neurotransmission in the murine gastric fundus. *J Physiol* 2013;**591**(12):2971–2986.
29. Gwilt CR, Donnelly LE, Rogers DF. The non-neuronal cholinergic system in the airways: an unappreciated regulatory role in pulmonary inflammation? *Pharmacol Ther* 2007;**115**(2):208–222.
30. Quinn DM. Acetylcholinesterase enzyme structure, reaction dynamics, and virtual transition stats. *Chem Rev* 1987;**87**(5):955–979.
31. Kajekar R, Rohde HK, Myers AC. The integrative membrane properties of human bronchial parasympathetic Ganglia neurons. *Am J Respir Crit Care Med* 2001;**164**(10): 1927–1932.
32. Tanahashi Y, Katsurada T, Inasaki N, et al. Further characterization of the synergistic activation mechanism of cationic channels by M-2 and M-3 muscarinic receptors in mouse intestinal smooth muscle cells. *Am J Physiol Cell Physiol* 2020;**318**(3):C514–C523.
33. Janssen LJ. T-type and L-type Ca^{2+} currents in canine bronchial smooth muscle: characterization and physiological roles. *Am J Physiol Cell Physiol* 1997;**272**(6): C1757–C1765.
34. Yamakage M, Chen X, Tsujiguchi N, Kamada Y, Namiki A. Different inhibitory effects of volatile anesthetics on T- and L-type voltage-depen- dent Ca^{2+} channels in porcine tracheal and bronchial smooth muscles. *Anesthesiology* 2001;**94**(4):683–693.
35. Janssen LJ. Ionic mechanisms and Ca^{2+} regulation in airway smooth muscle contraction: do the data contradict dogma? *Am J Physiol Lung Cell Mol Physiol* 2002;**282**(6): L1161–L1178.
36. Perez-Zoghbi JF, Karner C, Ito S, Shepherd M, Alrashdan Y, Sanderson MJ. Ion channel regulation of intracellular calcium and airway smooth muscle function. *Pulm Pharmacol Ther* 2009;**22**(5):388–397.
37. Fleischmann BK, Wang YX, Kotlikoff MI. Muscarinic activation and calcium permeation of nonselective cation currents in airway myocytes. *Am J Physiol Cell Physiol* 1997;**272**(1):C341–C349
38. Tsvilovskyy VV, Zholos AV, Aberle T, et al. Deletion of TRPC4 and TRPC6 in mice impairs smooth muscle contraction and intestinal motility in vivo. *Gastroenterology* 2009;**137**(4): 1415–1424.
39. Wang YX, Zheng YM. Molecular expression and functional role of canonical transient receptor potential channels in airway smooth muscle cells. *Adv Exp Med Biol* 2011;**704**: 731–47.
40. Bolton TB. Role of electrogenic sodium pumping in response of smooth-muscle to acetylcholine. *J Physiol* 1973;**228**(3): 713–731.
41. Unno T, Komori S, Ohashi H. Inhibitory effect of muscarinic receptor activation on Ca^{2+} channel current in smooth muscle cells of guinea-pig ileum. *J Physiol* 1995;**484**(3) (Pt 3):567–581.
42. Melchiorre C, Angeli P, Lambrecht G, Mutschler E, Picchio MT, Wess J. Antimuscarinic action of methoctramine, a new cardioselective M-2 muscarinic receptor antagonist, alone and in combination with atropine and gallamine. *Eur J Pharmacol* 1987;**144**(2):117–124.
43. Caulfield MP. Muscarinic receptors-characterization, coupling and function. *Pharmacol Ther* 1993;**58**(3):319–379.
44. Jakubík J, Zimčík P, Randáková A, Fuksová K, El-Fakahany EE, Doležal V. Molecular mechanisms of methoctramine binding and selectivity at muscarinic acetylcholine receptors. *Mol Pharmacol* 2014;**86**(2):180–192.